Journal of Applied Polymer Science

Effect of Seed Characteristics on Morphology Development in Poly(*n*-butyl acrylate)-Poly(*n*-butyl methacrylate) Core-Shell Dispersions

Kattimuttathu I. Suresh,[1,2] Eckhard Bartsch[2,3]

[1]Polymers & Functional Materials Division, Indian Institute of Chemical Technology, Hyderabad, Andhra Pradesh 50007, India
[2]Institut für Makromolekulare Chemie, Albert-Ludwigs-Universitaet Freiburg, Stefan-Meier-Strasse 31, D-79104 Freiburg, Germany
[3]Institut für Physikalische Chemie, Albert-Ludwigs Universitaet Freiburg, Albert-Strasse 21, D-79104, Freiburg, Germany

Correspondence to: K. I. Suresh (E-mail: kisuresh@iict.res.in) or E. Bartsch (E-mail: eckhard.bartsch@physchem.uni-freiburg.de)

ABSTRACT: This article reports on the influence of synthesis characteristics such as seed cross linking, particle-size distribution (PSD), and surfactant in the seeded emulsion polymerization of *n*-butyl acrylate–butyl methacrylate core-shell systems. These systems were studied using a combination of techniques such as light scattering (static and dynamic), asymmetric field flow fractionation coupled with multiangle laser light scattering and transmission electron microscopy. Complimentary data, obtained from static light scattering and electron microscopy studies, on the effect of seed crosslinking on morphology development reveals that the presence of a crosslinked seed favors the formation of nonequilibrium core-shell morphology. For uncrosslinked seeds occluded structures were present with a diffuse boundary between the core and the shell. In both cases, i.e., with or without surfactant, a monomodal PSD was observed for the core-shell systems and the relative size polydispersity and the shape of the seed PSD were retained. Use of surfactant was found to broaden the PSD but did not seem to affect the formation core-shell morphology. The study also shows the influence of crosslinked seeds on the film properties. © 2012 Wiley Periodicals, Inc. J. Appl. Polym. Sci. 000: 000–000, 2012

KEYWORDS: seeded emulsion polymerization; cross linked seeds; morphology; static light scattering; particle-size distribution

Received 16 December 2011; accepted 10 April 2012; published online
DOI: 10.1002/app.37858

INTRODUCTION

The past few decades have witnessed a growing concern for the environment, that is driving the development of new technologies for the coating industry. One of the means to address the environmental pollution problem is by replacing solvent-based coating technologies with water borne systems.[1,2] However, even with water-based systems, volatile organics are used to promote coalescence during film formation. They lower the modulus of the latex polymer to promote particle deformation during drying and the final film properties are achieved on evaporation of the volatile organic compound. Strategies such as blending of hard and soft colloidal dispersions facilitate film formation of aqueous latex dispersions without the need for any volatile organic additives.[3–6] A requirement for these type of systems is that the hard latex be sufficiently small and well dispersed within the matrix of the soft polymer and the refractive index of the two latex polymers be similar, thus reducing the number of candidate materials.

Designing structured polymer particles with core shell morphology is an efficient alternative to physical blending of different latices with additional advantages such as good dispersion of the constituents and better control of minimum film formation temperature (MFFT). Compared to materials made by copolymerization or blending, core shell particles of well defined morphology have unique physical properties and are studied widely.[7–14] Depending upon the design parameters, particles with such well-defined morphology have important applications, ranging from adhesives and coatings to impact modifiers in brittle plastics.[15] Over the years quantitative guidelines and predictive methods were developed for estimating the equilibrium morphology.[13,16,17] Formulation parameters considered to be important in controlling the particle morphology and final properties are surfactants,[18,19] initiators,[20,21] polymer type,[16] and crosslinking of the seed polymer.[22–24] The choice of a particular monomer is normally dictated by the end use application. *n*-butyl acrylate (BA) is an industrially important monomer and its emulsion polymerization and film formation from latices have been extensively studied, either alone[25–28] or in copolymerization with styrene (St),[29] methyl methacrylate (MMA)[30,31] and butyl methacrylate (BMA),[32] to produce

materials having the glass transition temperature or other properties in the desired range. To the best of our knowledge, the effect of crosslinking on the morphology development in the PBA-PBMA system has not been reported.

Two important parameters influencing the nonequilibrium morphology development in core-shell particles are the monomer type as well as crosslinking. Crosslinking also has an influence on many technological properties of the final film such as stiffness, toughness, barrier properties, etc.[22–24] The monomer BA crosslinked with ethylene glycol diacrylate (EGDA) was chosen for the good reactivity of its second vinyl function and also its chemical similarity to BA, which result in a homogenously crosslinked seed. *n*-BMA was chosen as the second monomer because its polymer has a higher T_g and is more hydrophobic relative to PBA. The objective of this work was to investigate the effect of seed characteristics and surfactant on core-shell (internal structure) morphology development and film properties of PBA-PBMA composite dispersions. This system was chosen because pure poly(butyl methacrylate) dispersions give brittle films at room temperature, due to the higher T_g, and pure poly(butyl acrylate) films are too tacky due to their low glass transition temperature.

EXPERIMENTAL

Materials

The monomer, *n*-butyl methacrylate, procured from Merck was distilled under vacuum in a nitrogen atmosphere and then stored at −18°C until use. The initiator, potassium persulfate ($K_2S_2O_8$), procured from Aldrich was used as such. Deionized water from a Millipore unit was used in all polymerization experiments after filtration through an ultra filtration unit of 0.1 μm pore size. Polymerizations were carried out at 78°C ± 2°C in a 250 mL round bottom flask fitted with a PTFE glass stirrer, gas bubbler, and a reflux condenser. Seed dispersions with varying degree of crosslinking were prepared from butyl acrylate monomer and EGDA crosslinker through a conventional batch emulsion polymerization process at a solid content of ~10% as reported earlier.[33] Typically 10 g of butyl acrylate with the required amount of EGDA crosslinker (e.g., 0.063 g EGDA for a 1 : 100 crosslinked seed) was polymerized in a 250 mL round bottom flask using potassium persulfate as initiator. The stirring speed was fixed at 250 rpm. Sodium dodecyl sulfate (SDS) was used as surfactant at a concentration of 0.28 g/100 mL. The polymerization was conducted for 24 h to achieve maximum conversion. Seed dispersions were also syntheiszed without any surfactant. The synthesized dispersions were filtered through a 0.25 μm nylon filter cloth and used as seed during the second stage of polymerization.

Core-Shell Dispersion Synthesis

The core-shell polymerizations were conducted using a semi-continuous batch process. Water and the seed dispersion were first charged into the reactor and heated to 78°C with continuous bubbling of argon. The initiator solution (0.05 g potassium persulfate in 10 mL water preheated to the reaction temperature) was then added. Within a few seconds addition of the second stage monomer was also started. The feeding rate was fixed in all the cases to 4.26–4.36 mL/h. No additional surfactant was used in the second stage. Samples were prepared at varying core-shell ratios using different seed dispersions. A typical recipe used for the synthesis is given in Table I.

Table I. Typical Recipe Used for the Preparation of Poly(butyl acrylate)–Poly(butyl methacrylate) Core-Shell Dispersions

Ingredients	Weight (g)
Poly(butyl acrylate) seed (~10% solids content)	50
Deionised water	50
Butyl methacrylate	5.15
K_2 S_2 O_8	0.050

Feeding rate 4.36 mL/h; temperature 78°C; stirring speed 250 rpm.

Characterization Methods

Determining the detailed morphology of composite latex particles, especially in cases where the difference in refractive index between the core-shell is negligible, in a confident manner is often very challenging and sometimes seemingly impossible. Complimentary sets of analytical data were shown to be helpful to determine the particle structure with confidence in such cases.[34] Thus, as discussed briefly in the following sections, we used a combination of different techniques for characterization of the core-shell dispersions.

Dynamic Light Scattering. Dynamic light scattering measurements for determination of particle size was performed with an ALV 5000 correlator from ALV, Langen, using a standard optical set up with a Nd-YAG solid state ring laser unit (DPSS-50; COHERENT), emitting green light of wavelength 532 nm. The results were analyzed using the cumulant method[35] yielding the hydrodynamic radius (R_H), from which the particle number of the colloids was calculated using the following expression.

$$N_p = \frac{6 \times 10^{21} \mathrm{SOC}}{\pi D_p^3 d} \tag{1}$$

Here N_p is the particle number per cubic centimeter (cc), D_p is the average particle diameter in nm, SOC is the solid content in g/mL and "d" is the polymer density in g/mL (taken as 1 g/mL in the present case). The final particle number of the seed dispersion was calculated using this equation to correct the particle number for coagulum formation.

For particles prepared with surfactant the surface coverage was calculated from the particle size data using the relation[33]:

$$\chi = \frac{F\langle R\rangle \rho_p a_m N_A}{3M_{\mathrm{emul}}} \tag{2}$$

here χ is the percent surfactant coverage, F denotes the mass ratio of emulsifier to monomer, $<R>$ is the average particle radius, M_{emul} is the emulsifier molecular weight, ρ_p is the polymer density, a_m gives the area occupied by a surfactant molecule on the particle surface and N_A is the Avogadro constant.

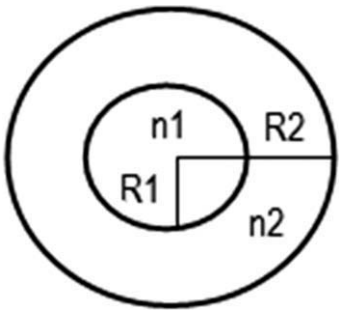

Figure 1. Two layer core-shell structure. Here, n1 and n2 represent the refractive index of the polymer forming the core and the shell having radii R_1 and R_2, respectively.

Asymmetric Field Flow Fractionation (AFFF). To characterize the particle-size distribution (PSD) of the dispersions the asymmetric FFF technique was used,[36–38] (see Ref. 37 for description of a standard experimental set up), because light scattering does not yield the PSD and the cumulant analysis cannot resolve small polydispersities well enough to capture secondary nucleation during core-shell synthesis. In this technique a field flow fractionation unit (AFFF, CONSENXUS), coupled with a multiangle laser light scattering (MALLS) set up[37] was used. In this method separation according to particle size is effected by a competing cross flow through a membrane and Brownian diffusion of the particles. Deionized water obtained from a Millipore unit was used as the solvent, to which 180 mg/L of salt and 30 mg/L of the surfactant Tween 20 were added. The fractionator used was a model F-100 from FFF fractionation, Salt Lake City. The 250 μm Teflon spacer (28.5 cm length 2.0 cm width) was surrounded by metal frits with a pore size of 3–5 μm.

The channel effluent was directed to the flow cell of a DAWN-DSP-F light scattering photometer (Wyatt Technology, Santa Barbara, CA). The light scattered from the flowing stream is detected using photo detectors placed around the flow cell to enable measurement over a range of angles (typically at 15–160 degrees). Each detector has its own integrated circuit for processing the analog signal. The digital output is transmitted to a computer. The data analysis and interpretation was achieved using ASTRA Software (Version 4.70). In principle, the radii distribution curves obtained from a FFF unit with MALLS give the fraction of the material with a particular radius. The radius distribution graphs as well as polydispersity were calculated from the data.

Static Light Scattering (SLS). The experimental setup used for measurement of particle size by dynamic light scattering was used in static light scattering as well. In static light scattering the angular profile of the scattered intensity is measured over a range of angles, usually from 30 to 150°, and information on the size and the internal structure of colloidal particles can be obtained through contrast variation.[39,40] This contrast is a quantitative difference between particles and solvent, characteristic for the type of radiation involved: a difference in electron density for X-rays, difference in scattering length density for neutrons or a difference in refractive index for light. Contrast variation is often applied within the Guinier approximation, i.e., the product of particle radius and scattering vector is small, on dilute suspensions.

For large particles with core-shell morphology the radius can be obtained from location of the common intersection point of intensity curves measured at different contrasts. It is also possible to determine the value of the refractive index of particles from the extrapolation of the intensity to zero at finite q. This concept was first applied to core-shell systems by Philipse et al.[39] assuming a schematic representation of the core-shell particles as in Figure 1.

The intensity profile (I_q) of scattered light from such a core-shell particle is given by eq. (3).

$$I(q) = (4\pi/q^3)^2\{(n_1 - n_2)[\sin(qR_1) - qR_1\cos(qR_1)] + (n_2 - n_s)[\sin(qR_2) - qR_2\cos(qR_2)]\}^2 \quad (3)$$

Here $q = (4\pi n_D/\lambda_0)\sin(\theta/2)$ is the magnitude of the scattering vector calculated from the vacuum light wavelength λ_0, the refractive index n_D of the dispersion medium and the scattering angle, θ. The method is applicable only to particles with hydrodynamic radius, $R_{H,}$ greater than 150 nm, because of the fact that for smaller particle the intensity minima falls outside of the measuring range of the optical setup.

Transmission Electron Microscopy. Transmission electron microscopy (TEM) analysis of the core shell particle was carried out on a PHILIPS (model EM420) machine at an accelerating voltage of 80–100 kv. Test specimens were prepared by placing a drop of diluted latex on a carbon coated copper grid and then allowing it to dry overnight at room temperature. To protect the dispersion particles from beam damage the dispersion samples were negatively stained with uranyl acetate.[41] The dried sample was placed in the instrument sample holder equipped with a cold stage unit, cooled by liquid N_2 at the outer end, maintaining a temperature of about 0°C at the locus of the sample.

RESULTS AND DISCUSSION

In this work synthesis and characterization of core-shell particles (composed of a poly(*n*-butyl acrylate) (PBA) core and a poly(*n*-butyl methacrylate) (PBMA) shell) prepared through a seeded semibatch emulsion process are reported. The main objective was to study the effect of synthesis parameters like crosslinking level, seed size and surfactant effect on the morphology development. The interfacial tensions between the polymers as well as between polymer and water are important parameters affecting morphology development. Free energy considerations are also important in predicting the morphology. According to Durant et al.,[22] the total free energy of a crosslinked seed particle is $G = G_s + G_e + G_o$. Here G_s is the interfacial energy, G_o is the reference state energy and G_e is the elastic energy stored in the particle. The elastic forces are dependent on four parameters: the temperature T, the number of repeating units between crosslink's, M_c/M (M_c is the molecular weight between crosslinks), the displacement gradient tensor, α and the stiffness "b" of the chain. Durant et al.[23] studied the PMMA-PS system with PMMA seeds of varying degree of

TABLE II Characteristics of Poly(butyl acrylate)–Poly(butyl methacrylate) Core-Shell Dispersions

Sample code	Seed characteristics			Core-shell ratio (wt %)	Core-shell, R_H (nm)		Shell thickness (nm)
	R_H (nm)	δ	Surfactant		Theory	Exp.	
Cs0	141	-	-	50/50	177	170	29
Cs1	111	1 : 100	-	50/50	144	137	26
Cs2	136	1 : 50	-	50/50	172	164	28
Cs3	162	1 : 10	-	50/50	208	211	49
Cs4	32	1 : 100	SDS	50/50	41	40	8
Cs5	35	1 : 50	SDS	50/50	45	41	6

δ, cross link density; EGDA, ethylene glycol diacrylate crosslinker was used in all cases; SDS, sodium dodecyl sulfate, R_H, hydrodynamic radius obtained from dynamic light scattering.

crosslinking. Modeling studies showed that the total energy was dependent on the interfacial tension at the polymer/water interface, (seed polymer/water interface) and the (polymer 2/water interface) according to eq. (4).[23]

$$\Delta Gs = 4\pi(r_s^3 + r_0^3)^{\frac{2}{3}}\left(\gamma\frac{p1}{w} - \gamma\frac{p2}{w}\right) + \gamma\frac{p1}{p2}(r_0^2 - r_s^2) \qquad (4)$$

Here $\gamma_{P1/w}$ is the interfacial tension at the polymer 1 (seed polymer)/water interface, $\gamma_{P2/w}$ is interfacial tension at the polymer 2 water interface and $\gamma_{P1/P2}$ is interfacial tension between the two polymers. In eq. (4), +ve values of ΔG_s predict that the core-shell structure is preferred while negative values predict that the inverted core-shell structure is preferred. Occluded structures are a special case of inverted core-shell structure with multiple inclusions to minimize the free energy.[22] The interfacial tensions of PBA and PBMA against water are reported to be 22 and 26 mN/m, respectively.[42] The interfacial tension between PBA(1) and PBMA(2) is 0.655 mN/m, calculated according to Wu's method.[43] The introduction of the hydrophilic crosslinker EGDA was expected to reduce the interfacial tension value of PBA. It is also important to mention that there will be a decrease in interfacial tension due to the initiator groups, but as both PBA and PBMA will have initiator derived end groups, the effect will essentially cancel out and the net effect can be assumed to be negligible. Thus, based on thermodynamic considerations, following Sundberg et al.,[22] one would expect that an inverted core-shell structure will be formed in the absence of seed crosslinking. The dramatic effect of PBA remaining in the interior can be expected already with low levels of crosslinking and at increased levels of crosslinking a core-shell structure with uniform boundary will be formed.

In the present work the seed particles were prepared in separate batch experiments and crosslinked with varying concentration of EGDA crosslinker to achieve different cross link densities. Thus seed particles of varying T_g values and degree of cross linking were obtained. The important seed characteristics along with the composition of the various core–shell dispersions synthesized are presented in Table II.

The same core-shell weight ratio (50 : 50) was used in all cases. Preliminary analysis of the particle size data (c.f. Table II) show that a core-shell type structure is obtained. It can be seen from Table II that for surfactant free systems (entry Cs1 to Cs3) the shell thickness increases as the crosslink density of the seed was increased, from 1 : 100 (i.e., 1 cross linker per 100 monomer units) to 1 : 10. Good agreement between the experimentally determined values and theoretically calculated value of particle size, from known monomer weight, density and conversion, was observed. The particle size of samples without any crosslinker falls in between that of Cs1 and Cs3. For core-shell particles prepared with surfactants, Cs4 and Cs5, no appreciable difference in particle size was observed unlike the surfactant free systems. The core shell structure was further analyzed using electron microscopy. Typical TEM pictures showing exemplarily the internal structure of the particles are given in Figure 2.

In Figure 2(a), a clear boundary between the core and shell was visible, but in images "b" and "c," where an uncrosslinked seed was used, the boundary between core and shell is irregular. These results can be analyzed in the light of observations made by Sundberg et al.[14,17] Crosslinking of the seed polymer creates elastic forces which compete with the interfacial forces in the control of morphology. The final particle structure is sensitive to the level of crosslinking which can easily dominate morphology control and film properties. Sundberg et al. studied the effect of second stage monomer feed rate and seed polymer T_g on the development of the core-shell morphology for the polystyrene (PS)-poly(methyl methacrylate) (PMMA) system. It was shown that with slower monomer feed rate PMMA exhibits less and less penetration by the second stage PS, consistent with a lowering of the polymer radical penetration ratio and a core-shell morphology resulted. Joensson et al.[44] concluded that limitations on polymer radical transport might be the cause of non-equilibrium structures and not limitations on monomer transport. In the case of semicontinuous batch polymerization, as in the present study, where the second stage monomer was fed to the seed latex at a controlled feed rate, the monomer concentration in the particle was maintained at a minimal value. The high local viscosity creates a kinetic barrier towards polymer chain radical diffusion and this increases the degree of phase separation. This effect of high local viscosity is expected to be even stronger in a crosslinked seed than in a low T_g uncrosslinked seed. Uncrosslinked PBA due to its very low T_g value

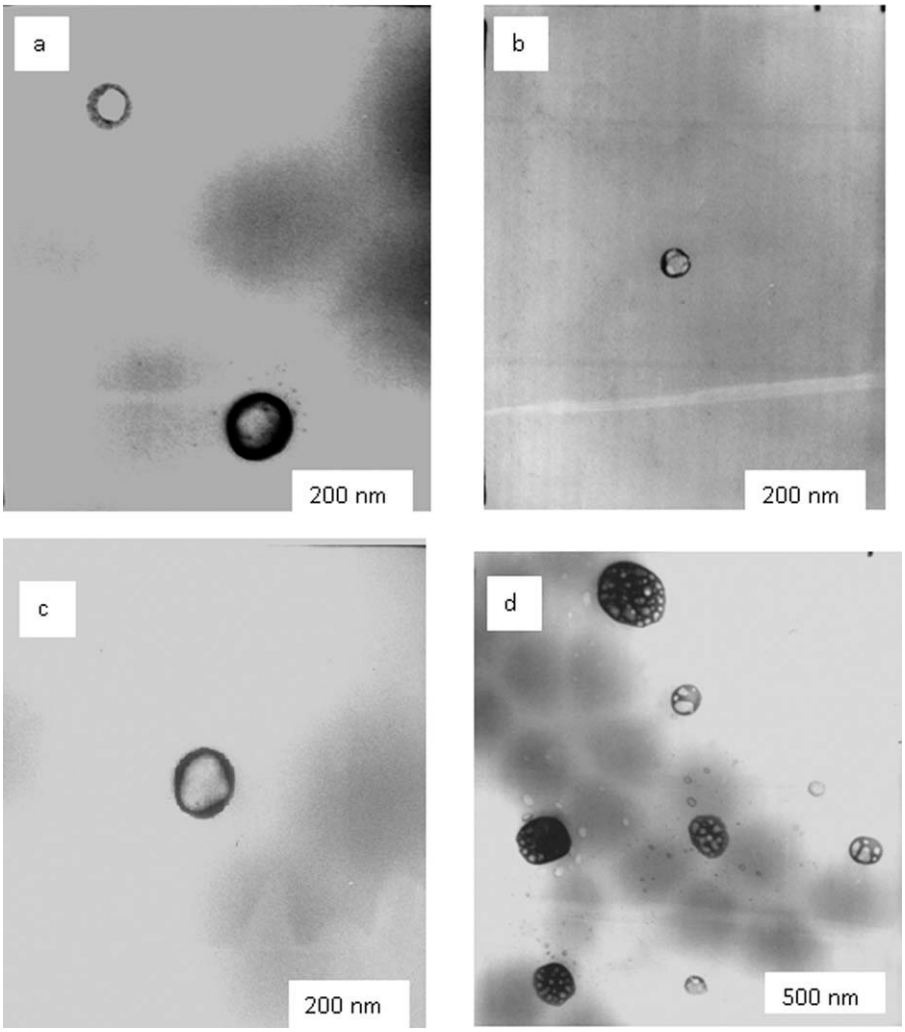

Figure 2. Transmission electron micrograph of PBA–PBMA core-shell latex particles with (a) 1 : 50 crosslinked core, (b, c) with uncrosslinked cores. Micrograph (d) shows occluded structures obtained when an uncrosslinked seed was used. In the images the light region corresponds to the PBA core and the dark region to the PBMA shell. The core shell weight ratio used in all cases was 1 : 1.

(−55°C) would allow for easy polymer radical penetration especially at the polymerization temperature, thus justifying the formation of occluded structures as well [cf. Figure 2(d)]. The light grey structure in the background [Figure 2(d)] may be due to a different particle layer and do not necessarily originate from the PBA cores alone.

Effect of Cross Linking on Morphology

To investigate the cross-linking effect, seed particles were prepared at varying crosslink densities, namely 1 : 10 (i.e., one crosslinker molecule for 10 monomer units), 1 : 50 and 1 : 100 using EGDA as the cross-linking agent. First, it is seen from Table II that the final particle size shows a clear dependence on the cross link density of the seed in a surfactant free polymerization [cf. Cs0–Cs3]. All the systems were prepared with 1 : 1 core-shell weight ratio and the particle size increased from 111 to 137 nm when a seed with 1 : 100 cross link density was used, i.e., a shell thickness of 26 nm resulted (cf. Table II, Cs1). When a seed of 1 : 10 cross link density was used, the particle size increases from 162 to 211 nm, giving a shell thickness of 49 nm. This is explained as follows: The second stage monomer was fed to the reactor in a semibatch fashion (4.24 mL/h) and the monomer concentration within the particles was maintained low throughout the reaction (starved feeding). The high local viscosity within the particle and the high instantaneous reaction rate (because of the starved feed conditions), both influence the morphology development.[44] For a tightly crosslinked seed either the monomer or the radicals cannot penetrate to the center of the particle.

Another explanation for this effect is that as the degree of cross linking increases the particle size of the seed increases[33] (i.e., the particle number decreases) and, consequently, during the second stage a greater shell thickness was obtained for the same monomer concentration, in going from Cs1 to Cs3. That is, the shell thickness obtained with a 1 : 100 EGDA crosslinked seed was 26 and 28 nm for a 1 : 50 crosslinked seed and 49 nm for a 1 : 10 crosslinked seed. The shell thickness for the system without any crosslinking was 29 nm, in between those with cross linked seeds, but here multiple occluded structures were formed

as indicated by the TEM studies. Comparison of surfactant free systems (Cs1 to Cs3) and SDS containing systems (Cs4 and Cs5) was expected to show the effect of particle size on core-shell morphology development. However, due to the very small size of the surfactant containing particles it was difficult to reach any conclusion with accuracy. The obtained values were well within the error of DLS measurement.

The existence of a diffusion process between the core and shell polymers is reflected in the film properties of the structured particles. According to Sundberg et al.,[17,22,23] to understand the effect of crosslinked seeds in the evolution of core-shell morphology, polymer radical diffusion rates and monomer diffusion rates have to be considered as the limiting factors. The work of Omi et al.[24] highlighted the dependence of the MFFT on EGDMA cross linked PBA seeds with either PMMA or PS shell. They observed an increase in MFFT with crosslinker concentrations up to 10 wt %, irrespective of whether a batch or a semibatch process was employed. In the present study, where a seed dispersion without any crosslinking was used (Cs0, Table II), the resulting core-shell dispersion gave flexible films (shore A hardness 24) at room temperature even though the PBMA shell T_g was higher than that of the core. This can be explained by assuming shell monomer diffusion into the core or vice versa, resulting in a lowering of the MFFT. In the absence of crosslinking, the low T_g poly(butyl acrylate) [−55°C] present in the core may diffuse to the outer shell material forming occluded structures, which further minimize the interfacial energy (as the interfacial tension of PBA/water is lower than that of PBMA/water).[42] This mixing increases the flexibility and tendency to form films at room temperature. The TEM pictures also showed that the dispersion particles have a diffuse boundary [c.f. Figure 2(b, c)]. Crosslinking affecting the diffusion process was also revealed from the work of Antonietti and coworkers.[45] They studied the internal structure of polystyrene microgel particles in a linear polystyrene matrix using small angle neutron scattering (SANS). It was shown that the micronetworks (crosslinked particles) form a relatively open structure with many internal loops and are freely interpenetrated by chains in the linear PS matrix, whereas interpenetration of chain segments was impeded in a pure micro network matrix without any linear polymer. The existence of diffusion mixing between PBA–PBMA phases was also observed by Duenas et al.[32] in an interpenetrating network system of these two polymers. The formation of nanoscale miscible domains was observed at lower cross-linking density.

With an increase in the degree of seed crosslinking [Cs1 to Cs3] the film formation ability of the dispersions at room temperature decreased as indicated by cracks in the film when the dispersion dries. This could be attributed to limited diffusion taking place between the core and shell on a micro scale. However, these particles form tough films (with Shore A hardness value 65) on annealing at 40°C, slightly above the T_g of the pure poly(butyl methacrylate). This shows that even when the cores [1 : 10 crosslinked] behave as hard spheres, the particles can deform sufficiently to give films where the core particles are distributed in a matrix formed by the shell polymer.

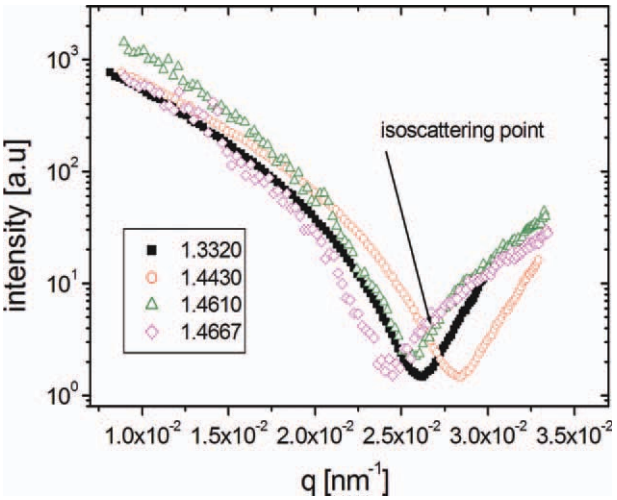

Figure 3. Semilogarithmic plot of scattered intensity versus scattering vector q for diluted PBA-PBMA core-shell particles (Cs2) in water–glycerol mixtures. The curves were labeled by the refractive index, n_s, of the solvent mixture. The location of the intersection point and of the minima gives information on the size and morphology, as explained in the text. [Color figure can be viewed in the online issue, which is available at wileyonlinelibrary.com.]

Static Light Scattering Studies

Further understanding of the effect of crosslinked cores on development of core-shell morphology comes from contrast variation studies using static light scattering. For contrast variation studies we selected the PBA-PBMA core-shell particles with 1 : 50 EGDA crosslinked core (Cs2) and with uncrosslinked core (Cs0). The contrast variation results for dilute suspension of the prepared core-shell particles (Cs2) in glycerol water mixture at varying contrast are shown in Figure 3. First, the intensity profile shows a minimum indicating that the particles were sufficiently large. Second, according to the theory of Philipse and coworkers[39] this profile changed markedly with the contrast, which points to inhomogeneous particles. The refractive index poly(butyl acrylate) was 1.466, while the value for poly(butyl methacrylate) was 1.483 at 20°C.[46]

The shift of the minima with the composition of the solvent mixture can be explained in terms of the two layer model proposed by Philipse et al. [cf. see experimental section, eq. (3)].[37] When the shell was matched in refractive index to that of the solvent there was only scattering from the core and the radii of the core can be measured from the corresponding minima. When the core is matched, there is only scattering from the shell. Another feature of the plot is that the curves measured at different contrasts intersect at a common point. This is called the isoscattering point, from which the particle radius can be calculated. The radius estimated from the isoscattering point was 170 nm, which is close to the dynamic light scattering radii of 164 nm [cf.Cs2 Table II.] The small difference could be due to the fact that actual concentrations were not measured but adjusted by the turbidity and scattering light intensity to facilitate measurements over the entire angular range. (The scattered intensity is proportional to the concentration and refractive index of solvent, i.e., $I \propto c\, n_s^2$).

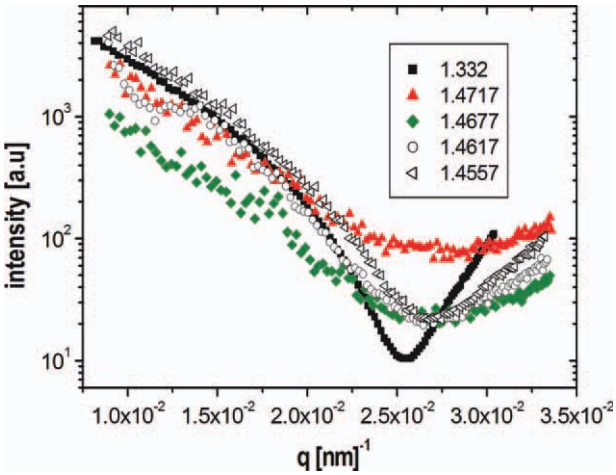

Figure 4. Particle form factor of PBA-PBMA core-shell particle Cs0 (with uncrosslinked core) in glycerol–water mixtures at varying refractive index values. The refractive index value (given in inset) was changed by adjusting the composition of the solvent system. [Color figure can be viewed in the online issue, which is available at wileyonlinelibrary.com.]

Shown in Figure 4 is the contrast variation study on the system without any seed cross linking. Here, no appreciable shift of the form factor minima was observed with varying contrast but a flattening of the minima. The scattering curve in water shows a noticeably different line shape and seems not to fit into the picture. Here, the minimum was significantly shifted to the left as compared to the other) curves while the latter appear to have their minima at the same *q*-value. This was attributed, most likely, as a consequence of Mie scattering, which comes into play when the refractive index of the solvent differs too much from that of the particles. The flattening of the minimum could be attributed to the fact that a sharp interface as depicted in the Figure 1 is not present in this system. There could be some miscibility between the core and shell polymers as suggested by the nearly similar values of the solubility parameter.[46] Thus, the contrast variation studies confirm that crosslinking enhances the phase separation and the formation of a core-shell structure as anticipated. If the particles are sufficiently large the static light scattering technique can be applied to gain information on the internal structure of core-shell particles. This interpretation was also supported by the TEM pictures given in Figure 2, where the boundary between core and shell appears non uniform for core-shell particles without any seed crosslinking, whereas a sharp interface was visible with crosslinked seeds.

Secondary Nucleation During Core-Shell Synthesis

Analyzing the particle number data calculated from measured particle sizes is a useful approach in qualitative assessment of core-shell structure development.[47,48] The assumption was that if all the monomers used in the second stage of the process do not form a shell but instead give rise to new particles that grow independently, then the particle number of the final systems will be significantly increased. The particle number was calculated before and after polymerization of the shell monomer using eq. (1). The results are plotted in Figure 5 for the core-shell systems prepared (a) in presence of SDS and (b) for the surfactant free systems. As seen from Figure 5(a), where SDS was used as the surfactant, the N_{new}/N_{seed} value varies between 1.0 and 1.14. For the 1 : 100 crosslinked seed (Cs4) no secondary nucleation was observed as N_{new}/N_{seed} was found to be 1.02. In contrast, the value of about 1.14 for the 1 : 50 crosslinked seed may suggest somesecondary nucleation. This was also reflected in the lower shell thickness obtained in this case (cf.Table II, Cs5) as compared to expectation based on results with the surfactant free system. Thus, the observed effect could only be due to the small size. The TEM studies with smaller core-shell particles showed that film formation takes place and the individual particles were not visible under the same conditions as used for sample preparation. This is in agreement with the hypothesis that smaller particles deform more easily than bigger ones.[49] For surfactant free systems, as seen from Figure 5(b), nearly all synthesized systems have a N_{new}/N_{seed} ratio of approximately unity, suggesting negligible secondary nucleation and the formation of a core-shell structure.

The observed results are in agreement with the work of Morrison and co workers who studied the effect of seed particle size on secondary nucleation in polystyrene latices.[47] The effect of seed particle number density for a given particle size was studied for systems with seed radii of 46, 110, and 192 nm. It was found that the smaller seed particles, of radii 46 nm, caused extensive secondary nucleation at a lower number density than bigger size seeds. In other words, small particles require a higher critical seed number density to prevent secondary nucleation. The seed dispersion with small particle was found to stop the formation of visible new particles at $\sim 10^{15}$ dm^{-3} of seed particles whereas for the largest seed particles examined, new nucleation was prevented at $\sim 10^{14}$ dm^{-3} of seed particles. In their system the surfactant concentration was below the critical micelle concentration. Thus, it appears that in our study, the seed number density of Cs5, may not be sufficient to prevent

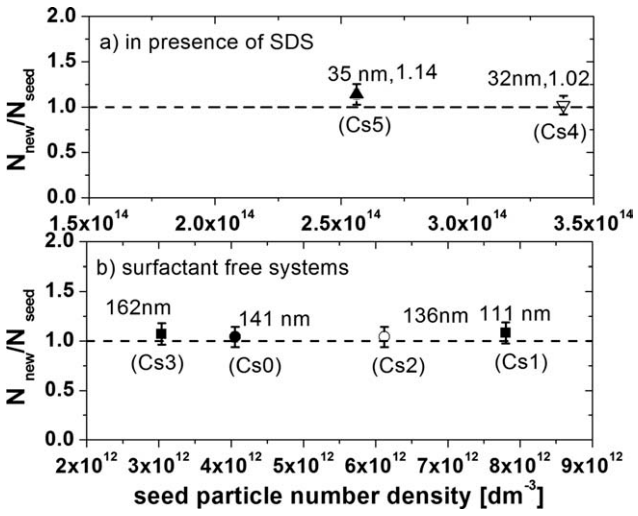

Figure 5. Effect of seed particle number density on secondary nucleation during the synthesis of PBA-PBMA core-shell particle emulsion. Only in (a) the N_{new}/N_{seed} values were indicated adjacent to the particle size, to avoid overcrowding (b) with numbers. All data points are marked with an error bar of 10%.

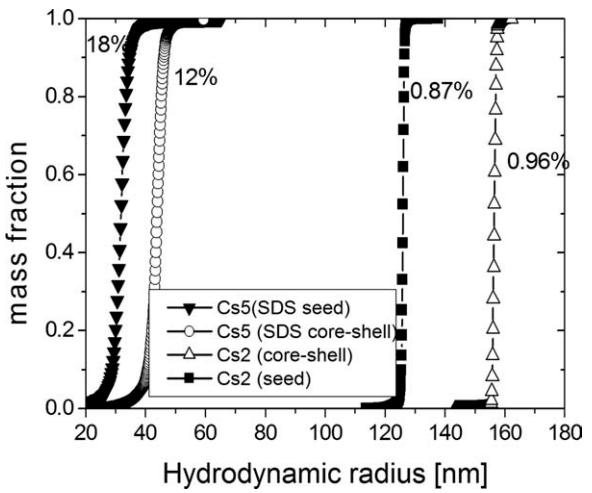

Figure 6. Particle size distribution of poly(butyl acrylate)-poly(butyl methacrylate) core-shell dispersions prepared with anionic surfactant SDS containing seed and a surfactant free seed. The numbers at the curves give the polydispersity.

secondary nucleation. During synthesis of the seed dispersion the SDS concentration used was just above its CMC (critical micelle concentration) and thus the free surfactant present in excess of CMC may be contributing to the mild secondary nucleation observed. Nevertheless, the TEM results and the PSD data (see later) support the formation of a core-shell structure.

Particle-Size Distribution

The influence of surfactant and crosslinker concentration on the PSD of the seed was earlier reported.[33] The PSD was obtained from the measured particle radii using AFFF. In Figure 6, the PSD of seed and core-shell dispersions prepared with and without surfactant were compared. The MALLS results show that core-shell systems prepared, either with surfactant or as surfactant free systems, have nearly identical PSD as that of the seed.

The presence of surfactant certainly had an influence on the PSD as the polydispersity values (cf. adjacent to the curves in Figure 6) suggest. The size distribution curves further show that there is no secondary distribution. When SDS was used as surfactant the seed emulsion was found to have a broader PSD (18%) than the core-shell system (12%). The distribution becomes narrow when the shell was formed. However, no bimodal distribution was observed, even in this case. Thus, the study of PSD also suggests formation of core-shell structure. Therefore, the only effect of surfactant on morphology of the structured particles could be the generation of new particles and this, if substantial, would affect the PSD to a noticeable extent or lead to a multimodal distribution and value of N_{new}/N_{seed} deviating from unity. To summarize, the PSD data suggests absence of secondary nucleation occurring during the core-shell synthesis in surfactant free systems. In the system prepared with SDS, the surfactant amount was less than what required for 100% coverage[33] of the seed particles. Thus, the effect of free surfactant causing secondary distribution was rather small.

CONCLUSIONS

The effect of seed crosslinking and SDS surfactant on size, morphology and size distribution of PBA-PBMA core-shell dispersions synthesized by seeded emulsion polymerization was studied. The size of the core-shell particles increased with increasing degree of seed crosslinking, an effect parallel to that observed during the preparation of the seed. The study of the PSDs by asymmetric field flow fractionation suggested that secondary nucleation in the seeded polymerizations was absent or below detection limit as all systems show monomodal PSDs. These results were also supported by the particle number data. Morphological studies using TEM shows that for uncrosslinked cores the boundary between the core and shell was not well defined. In contrast, a clear boundary between core and shell was visible, when a crosslinked seed was used. Detailed analysis of the core-shell structure using static light scattering through contrast variation indicated that a crosslinked seed facilitated the formation of core-shell morphology with defined boundaries. The film properties, such as flexibility and clarity, were in addition influenced by seed size and crosslinking. For example, the films prepared with 1 : 10 crosslinked seeds were tough and partly opaque, whereas flexible and near transparent films were obtained with uncrosslinked or 1 : 100 crosslinked seed.

ACKNOWLEDGMENTS

The financial support from DAAD (Deutscher Akademischer Austausch Dienst to K. I. Suresh under CSIR-DAAD Exchange program is gratefully acknowledged. The authors thank Michael Drahus for the critical reading of the manuscript.

REFERENCES

1. Karsa, D. R. Additives for Water based Coatings; Royal Chemical Society: London, **1990.**
2. Winnik, M. A.; Wang, Y.; Haley, F. J. *J. Coat. Tech.* **1992,** *64*, 51.
3. Colombini, D.; Hassander, H.; Karlsson, O. J.; Maurer, F. H. *J. Macromolecules* **2004,** *37*, 6865.
4. Feng, J.; Winnik, M. A.; Shivers, R.; Clubb, B. *Macromolecules* **1995,** *28*, 7671.
5. Patel, A. A.; Feng, J.; Winnik, M. A.; Mcbain, C. D. *Polymer* **1996,** *37*, 5577.
6. Winnik, M. A.; Feng, J. J. *Coat. Technol.* **1996,** *68*, (852), 39.
7. Kirsch, S.; Doerk, A.; Bartsch, E.; Sillescu, H. *Macromolecules* **1999,** *32*, 4508.
8. Dimonie, V.; El-Aasser, M. S.; Klein, A.; Vanderhoff, W. J. *J. Polym. Sci. Part A: Polym. Chem.* **1984,** *22*, 2197.
9. Okubo, M. *Makromol. Chem. Makromol. Symp.* **1990,** *35*, 307.
10. Cho, I.; Lee, R. W. *J. Appl. Polym. Sci.* **1985,** *30*, 1903.
11. Lee, D. I.; Ishikawa, T. J. *J. Polym. Sci. Part A: Polym. Chem.* **1983,** *21*, 147.
12. Karlsson, O. J.; Hassander, H.; Colombini, D. C. *R. Chimie* **2003,** *6*, 1233.

13. Sundberg, D. C.;Casacca, A. P.; Pantazopoulos, J.; Muscato, M. R.; Kronberg, B.; Berg, J. J. *Appl. Polym. Sci.* **1990,** *41*, 1425.
14. Ivarsson, L. E.; Karlsson, O. J.;Sundberg, D. C. *Macromol. Symp.* **2000,** *151*, 407.
15. Blankenship, R.; Kowalski, A. *U.S. Pat. 4,594,*363 (**1986**).
16. Sundberg, E. J.; Sundberg, D. C. *J. Appl. Polym. Sci.* **1993,** *47*, 1277.
17. Stubbs, J.; Karlsson, O.; Joenson, J.; Sundberg, E.; Durant, Y.; Sundberg, D. *Colloids Surf. A: Physchem. Eng.* **1999,** *153*, 255.
18. Chen, Y. C.; Dimonie, V.; El-Aasser, M. S. *J. Appl. Polym. Sci.* **1992,** *45*, 487.
19. Lee, S.; Rudin, A. *Makromol. Chem. Rapid Commun.* **1989,** *10*, 655.
20. Lee, S.; Rudin, A. J. *Polym. Sci. Part A: Polym. Chem.* **1992,** *30*, 2211.
21. Stubbs, J. M.; Sundberg, D. C. *J. Appl. Polym. Sci.* **2004,** *91*, 1538.
22. Durant, Y. G.; Sundberg, E. J.; Sundberg, D. C. *Macromolecules* **1996,** *29*, 8466.
23. Durant, Y. G.; Sundberg, E. J.; Sundberg, D. C. *Macromolecules* **1997,** *30*, 1028.
24. Omi, S.; Kohmoto, T.; Iso, M. *Polym. Int.* **1993,** *30*, 499.
25. Maeder, S.; Gilbert, R. G. *Macromolecules* **1998,** *31*, 4410.
26. Potisk, P.; Capek, I. *Angew. Macromol. Chem.* **1994,** *218*, 53.
27. Plessis, C.; Arzamendi, G.; Leiza, J. R.; Schoonbrood, H. A. S.; Charmot, D.; Asua, J. M. *Macromolecules* **2000,** *33*, 5041.
28. Sajjadi, S.; Brooks, B. W. *J. Appl. Polym. Sci.* **1999,** *74*, 3094.
29. Silverstein, M.; Talmon, Y.; Narkis, M. *Polymer* **1989,** *30*, 416.
30. Kirsch, S.; Pfau, A.; Landfester, K.; Shaffer, O.; El-Aasser, M. S. *Macromol. Symp.* **2000,** *151*, 413.
31. Santos, F. D. D.; Farbe, P.; Dryon, X.; Meunier, G.; Leibler, L. J. *Polym. Sci. Part B: Polym. Phys.* **2000,** *38*, 2989.
32. Duenas, J. M. M.; Escuriola, D. T.; Ferrer, G.; Pradas, M. M.; Ribelles, J. L. G. *Macromolecules* **2001,** *34*, 5525.
33. Suresh, K. I.; Othegraven, J.; Raju, K. V. S. N.; Bartsch, E. *Colloid Polym. Sci.* **2004,** *283*, 49.
34. Stubbs, J. M.; Sundberg, D. C. *Polymer* **2005,** *46*, 1125.
35. Koppel, D. E. *J. Chem. Phys.* **1972,** *57*, 4814.
36. Tank, C.; Antonieti, M. *Macromol. Chem. Phys.* **1996,** *197*, 2943.
37. Bartsch, S.; Kulicke, W. M.; Fresen, I.; Moritz, H.-U. *Acta Polym.* **1999,** *50*, 373.
38. Cölfen, H.; Antonietti, M. *Adv. Polym. Sci.* **2000,** *150*, 67.
39. Philipse, A. P.; Smits, C. S.; Vrij, A. J. *Colloid Interface Sci.* **1989,** *129*, 335.
40. Bryant, G.; Mortensen, T.; Henderson, S.; Williams, S.; van Megen, W. J. *Colloid Interface Sci.* **1999,** *216*, 401.
41. Kirsch, S.; Landfester, K.; Shaffer, O.; El-Aasser, M. S. *Acta Polym.* **1998,** *50*, 347.
42. Dong, Y.; Sundberg, D. C. *J. Colloid Interface Sci.* **2003,** *258*, 97.
43. Wu, S. J. *Polym. Sci. Part C* **1971,** *34*, 19.
44. Jönsson, J. E.; Hassander, H.; Jansson, L. H.; Törnel, B. *Macromolecules* **1994,** *27*, 1932.
45. Antonietti, M.; Ehlich, D.; Foelsch, K. J.; Sillescu, H.; Schmidt, M.; Lindner, P. *Macromolecules* **1989,** *22*, 2802.
46. Brandrup, J.; Immergut, E. H., Polymer Hand Book, 2nd ed.; Wiley: New York, **1974.**
47. Morrison, B. R.; Gilbert, R. G. *Macromol. Symp.* **1995,** *92*, 13.
48. Ferguson, C. J.; Russel, G. T. *Gilbert, R. G. Polymer* **2002,** *43*, 4551.
49. Meincken, M.; Sanderson, R. D. *Polymer* **2002,** *43*, 4947.